Monte Carlo simulations of an unconventional phase transition for a two-dimensional dimerized quantum Heisenberg model

F.-J. Jiang

Phys. Rev. B **85**, 014414 — Published 17 January 2012

DOI: 10.1103/PhysRevB.85.014414

Monte Carlo simulations of an unconventional phase transition for a 2d dimerized quantum Heisenberg model

F.-J. Jiang[1, *]

[1]*Department of Physics, National Taiwan Normal University, 88, Sec.4, Ting-Chou Rd., Taipei 116, Taiwan*

Motivated by the indication of a new critical theory for the spin-1/2 Heisenberg model with a spatially staggered anisotropy on the square lattice, we re-investigate the phase transition of this model induced by dimerization using first principle Monte Carlo simulations. We focus on studying the finite-size scaling of $\rho_{s1}2L$ and $\rho_{s2}2L$, where L stands for the spatial box size used in the simulations and ρ_{si} with $i \in \{1, 2\}$ is the spin-stiffness in the i-direction. Remarkably, while we observe a large correction to scaling for the observable $\rho_{s1}2L$, the data for $\rho_{s2}2L$ exhibit a good scaling behavior without any indication of a large correction. As a consequence, we are able to obtain a numerical value for the critical exponent ν which is consistent with the known $O(3)$ result with moderate computational effort. Further, we additionally carry out an unconventional finite-size scaling analysis with which we assume that the ratio of the spatial winding numbers squared is fixed through all simulations. The theoretical correctness of our idea is argued and its validity is confirmed. Using this unconventional finite-size scaling method, even from $\rho_{s1}L$ which receives the most serious correction among the observables considered in this study, we are able to arrive at a value for ν consistent with the expected $O(3)$ value. A detailed investigation to compare these two finite-size scaling methods should be performed.

PACS numbers:

I. INTRODUCTION

Heisenberg-type models have been one of the central research topics in condensed matter physics during the last two decades. The reason that these models have triggered great theoretical interest is twofold. First of all, Heisenberg-type models are relevant to real materials. Specifically, the spin-1/2 Heisenberg model on the square lattice is the appropriate model for understanding the undoped precursors of high T_c cuprates (undoped antiferromagnets). Second, because of the availability of efficient Monte Carlo algorithms as well as the increased power of computing resources, properties of undoped antiferromagnets on geometrically non-frustrated lattices can be simulated with unprecedented accuracy[1–15]. As a consequence, these models are particular suitable for examining theoretical predictions and exploring ideas. For instance, Heisenberg-type models are often used to examine field theory predictions regarding the universality class of a second order phase transition[11,14–19]. Furthermore, a new proposal of determining the low-energy constant, namely the spinwave velocity c of antiferromagnets with $O(2)$ and $O(3)$ symmetry, through the squares of temporal and spatial winding numbers was verified to be valid and this idea has greatly improved the accuracy of the related low-energy constants[20,21]. On the one hand, Heisenberg-type models on geometrically non-frustrated lattices are among the best quantitatively understood condensed matter physics systems; on the other hand, despite being well studied, several recent numerical investigation of spatially anisotropic Heisenberg models have led to unexpected results[14,22,23]. In particular, Monte Carlo evidence indicates that the anisotropic Heisenberg model with staggered arrangement of the antiferromagnetic couplings may belong to a new universality class, in contradiction to the theoretical $O(3)$ universality prediction[14]. For example, while the most accurate Monte Carlo value for the critical exponent ν in the $O(3)$ universality class is given by $\nu = 0.7112(5)$[24], the corresponding ν determined in[14] is $\nu = 0.689(5)$. Although the subtlety of calculating the critical exponent ν from performing finite-size scaling analysis has been demonstrated for a similar anisotropic Heisenberg model on the honeycomb lattice[25], the discrepancy between $\nu = 0.689(5)$ and $\nu = 0.7112(5)$ observed in[14,24] remains to be understood.

In order to clarify this issue further, theoretical effort has been devoted to studying the phase transition of this model induced by dimerization. Specifically, in[26] it is argued that the correction to scaling for this phase transition is enhanced because of a cubic irrelevant term, hence leads to the unexpected $\nu = 0.689(5)$ obtained in[14]. Although Monte Carlo results obtained at finite temperature seem to support this scenario of an enhanced correction to scaling, direct numerical evidences to solve this puzzle is not available yet. In this study, we undertake the challenge of determining the critical exponent ν by simulating the spin-1/2 Heisenberg model with a spatially staggered anisotropy on the square lattice. The relevant observables considered in this study for calculating the critical exponent ν are $\rho_{s1}2L$, $\rho_{s2}2L$ and Q_2. Here ρ_{si} with $i \in \{1, 2\}$ is the spin stiffness in the i-direction, L is the box size used in the simulations and Q_2 is the second Binder ratio which will be defined later. Further, we analyze in more detail the finite-size scaling of $\rho_{s1}2L$ and $\rho_{s2}2L$. The reason that $\rho_{s1}2L$ and $\rho_{s2}2L$ are chosen is twofold. First of all, these two observables can be calculated to a very high accuracy using loop algorithms[1,3,27,28]. Second, one can measure ρ_{s1} and ρ_{s2} separately. On isotropic systems, one would naturally

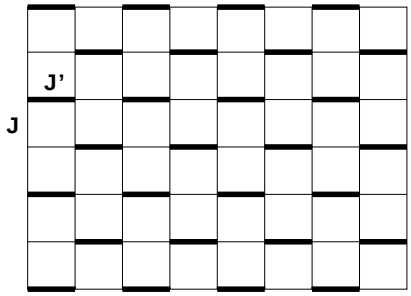

FIG. 1: The spatially anisotropic Heisenberg model considered in this study.

use ρ_s, which is the average of ρ_{s1} and ρ_{s2}, for the data analysis. However, for the anisotropic model considered here, we find it is useful to analyze both the data of ρ_{s1} and ρ_{s2} because such a study may reveal the impact of anisotropy on the system. Surprisingly, as we will show later, the observable $\rho_{s2}2L$ receives a much less severe correction than $\rho_{s1}2L$. Hence $\rho_{s2}2L$ is a better suited quantity than $\rho_{s1}2L$ for the finite-size scaling analysis. Indeed, with moderate computational effort, we can obtain a numerical value for ν consistent with the most accurate $O(3)$ Monte Carlo result $\nu = 0.7112(5)$. Beside the conventional finite-size scaling method, we additionally perform another unconventional analysis with which the aspect ratio of the spatial winding numbers squared is fixed. Remarkably, while from $\rho_{s1}2L$ we cannot obtain a numerical value for ν which agrees with the established $O(3)$ result using the conventional finite-size scaling method, we are able to reach a result from the same observable consistent with $\nu = 0.7112(5)$ by employing our unconventional method of fixing the aspect ratio of spatial winding numbers squared. Although for anisotropic systems and for the observables $\rho_{si}L$ with $i \in \{1, 2\}$, one can argue theoretically that the unconventional method we use is the correct approach for performing finite-size scaling, still, we can arrive at a correct value for ν from $\rho_{s2}2L$ using the conventional method. Further, since the conventional method has successfully led to correct determination of some critical exponents for anisotropic systems[10,15,25], it will be desirable to examine the results obtained from these two methods in a more detailed manner.

This paper is organized as follows. First, the anisotropic Heisenberg model and the relevant observables studied in this work are briefly described after which we present our numerical results. In particular, both the results obtained from the conventional and unconventional finite-size scaling methods are discussed in detail. A final section then concludes our study.

II. MICROSCOPIC MODEL AND CORRESPONDING OBSERVABLES

The Heisenberg model considered in this study is defined by the Hamilton operator

$$H = \sum_{\langle xy \rangle} J\, \vec{S}_x \cdot \vec{S}_y + \sum_{\langle x'y' \rangle} J'\, \vec{S}_{x'} \cdot \vec{S}_{y'}, \tag{1}$$

where J and J' are antiferromagnetic exchange couplings connecting nearest neighbor spins $\langle xy \rangle$ and $\langle x'y' \rangle$, respectively. Figure 1 illustrates the model described by Eq. (1). To study the critical behavior of this model near the transition driven by the anisotropy, in particular, to determine the critical point as well as the critical exponent ν, the spin stiffnesses in the 1- and 2-directions which are defined by

$$\rho_{si} = \frac{1}{\beta L^2} \langle W_i^2 \rangle, \tag{2}$$

are measured in our simulations. Here β is the inverse temperature and L again refers to the spatial box size. Further $\langle W_i^2 \rangle$ with $i \in \{1, 2\}$ is the winding number squared in the i-direction. In addition, the second Binder ratio Q_2, which is defined by

$$Q_2 = \frac{\langle (m_s^z)^2 \rangle^2}{\langle (m_s^z)^4 \rangle}, \tag{3}$$

is also measured in our simulations as well [1]. Here m_s^z is the z-component of the staggered magnetization $\vec{m}_s = \frac{1}{L^2} \sum_x (-1)^{x_1+x_2} \vec{S}_x$. By carefully investigating the spatial volume and the J'/J dependence of $\rho_{si}L$ as well as Q_2, one can determine the critical point and the critical exponent ν with high precision.

III. DETERMINATION OF THE CRITICAL POINT AND THE CRITICAL EXPONENT ν

In this section, the critical exponent ν as well as the critical point are determined by fitting the Monte Carlo data to their expected finite-size scaling ansatz. First of all, Let us focus on our results obtained by performing the conventional finite-size scaling.

A. Results from the conventional finite-size scaling analysis

To study the quantum phase transition, we have carried out large scale Monte Carlo simulations using a loop algorithm. Further, to calculate the relevant critical exponent ν and to determine the location of the critical

[1] Notice the conventional definition of Q_2 in the literature is given by $Q_2 = \langle (m_s^z)^4 \rangle / \langle (m_s^z)^2 \rangle^2$.

observable	L	ν	$(J'/J)_c$	χ^2/DOF
$\rho_{s2}2L$	$48 \le L \le 96$	0.7150(28)	2.51951(8)	1.0
$\rho_{s2}2L^\star$	$48 \le L \le 96$	0.7095(32)	2.51950(8)	0.9
$\rho_{s2}2L$	$48 \le L \le 136$	0.7120(16)	2.51950(3)	1.1
$\rho_{s2}2L$	$60 \le L \le 136$	0.7120(18)	2.51950(3)	1.1
$\rho_{s2}2L$	$66 \le L \le 136$	0.7125(20)	2.51950(4)	1.1
$\rho_{s2}2L^\star$	$48 \le L \le 136$	0.7085(16)	2.51950(3)	0.9
$\rho_{s2}2L^\star$	$60 \le L \le 136$	0.7087(17)	2.51950(3)	0.9
$\rho_{s2}2L^\star$	$66 \le L \le 136$	0.7096(19)	2.51950(4)	0.9
$\rho_{s1}2L$	$24 \le L \le 80$	0.689(3)	2.5194(4)	1.2
$\rho_{s1}2L^\star$	$24 \le L \le 80$	0.683(4)	2.5194(3)	1.1
$\rho_{s1}2L$	$48 \le L \le 136$	0.701(3)	2.5194(3)	1.6
Q_2	$48 \le L \le 136$	0.7116(50)	2.51952(8)	1.4
$Q_2^\star$	$48 \le L \le 136$	0.7050(48)	2.51950(8)	1.3

TABLE I: The numerical values for ν and $(J'/J)_c$ calculated from $\rho_{s2}2L$, $\rho_{s1}2L$ and Q_2. All results are obtained using a second order Taylor series expansion of Eq. (5), except those with a star, which are determined using an expansion to third order. The confluent correction ω is included in the fit explicitly only for $\rho_{s1}2L$.

point in the parameter space J'/J, we have employed the technique of finite-size scaling for certain observables. For example, if the transition is second order, then near the transition the observable $\rho_{si}2L$ for $i \in \{1,2\}$ and Q_2 should be described well by the following finite-size scaling ansatz[229–33]

$$\begin{aligned}\mathcal{O}_L(t) &= g_{\mathcal{O}}(tL^{1/\nu}, L^z/\beta, r) + L^{-\omega} g_{\mathcal{O}_\omega}(tL^{1/\nu}, L^z/\beta, r) \\ &= g_{\mathcal{O}}(tL^{1/\nu}, L^z/\beta, r) \times \\ &\quad \Big(1 + L^{-\omega} g'_{\mathcal{O}_\omega}(tL^{1/\nu}, L^z/\beta, r)\Big) \end{aligned} \tag{4}$$

where $\mathcal{O}_L$ stands for Q_2 and $\rho_{si}L$ with $i \in \{1,2\}$, L is the lattice size in the 1-direction, $t = (j_c - j)/j_c$ with $j = (J'/J)$, ν is the critical exponent corresponding to the correlation length ξ, ω is the confluent correction exponent, z is the dynamical critical exponent which is 1 for the phase transition considered here and r is the ratio of the lattice size in the 1- and 2-direction. Further, $g_{\mathcal{O}}$, $g_{\mathcal{O}_\omega}$ and $g'_{\mathcal{O}_\omega}$ appearing above are smooth functions of the variables $tL^{1/\nu}$, L/β and r. Using the full ansatz Eq. (4) for finite-size scaling will certainly introduce more unknown parameters, hence might lead to difficulty in estimating the errors accurately[3]. As a result, in practice one would carry out the analysis closes to the critical point so that $g'_{\mathcal{O}_\omega}$ in Eq. (4) can be approximated by a constant. Specifically the following ansatz

$$\mathcal{O}_L(t) = (1 + bL^{-\omega}) g_{\mathcal{O}}(tL^{1/\nu}, L^z/\beta, r), \tag{5}$$

where b is some constant, is frequently used when applying the finite-size scaling technique. While Eq. (5) is only valid for large box sizes and close to the critical point, to present the main results of this study we find it is sufficient to employ Eq. (5) for the data analysis. Notice that for square lattices, one will intuitively neglect the effect of r in Eq. (5). From Eq. (5), one concludes that the curves for $\mathcal{O}_L$ corresponding to different L, as functions of J'/J, should intersect at the critical point $(J'/J)_c$ for large L. To calculate the critical exponent ν and the critical point $(J'/J)_c$, in the following we will apply the finite-size scaling formula, Eq. (5) with $r = 1$, to the observables $\rho_{s1}2L$, $\rho_{s2}2L$ as well as Q_2. Without loss of generality, we have fixed $J = 1$ in our simulations and have varied J'. Additionally, the box size used in the simulations ranges from $L = 16$ to $L = 136$. To reach a lattice size as large as possible, we use $\beta J = 2L$ for each L in our simulation. As a result, the temperature dependence in Eq. (5) drops out. Figure 2 shows the Monte Carlo data for $\rho_{s1}2L$, $\rho_{s2}2L$ and Q_2 as functions of J'/J. The figure clearly indicates that the phase transition is most likely second order since for all the observables $\rho_{s1}2L$, $\rho_{s2}2L$ and Q_2, the curves of different L tend to intersect near a particular point in the parameter space J'/J. The most striking observation from our results is that the observable $\rho_{s1}2L$ receives a much more severe correction than $\rho_{s2}2L$. This can be understood from the trend of the crossing among these curves for different L near the transition (figure 3). Therefore one expects that a better determination of ν can be obtained by applying the finite-size scaling ansatz Eq. (5) to $\rho_{s2}2L$. Before presenting our results, we would like to point out that data from large volumes are essential in order to determine the critical exponent ν accurately as was emphasized in[25]. We will use the strategy employed in[25] for our data analysis as well. Let us first focus on $\rho_{s2}2L$ since this observable shows a good scaling behavior. Notice from figure 3, the trend of crossing for different L of $\rho_{s2}2L$ indicates that the confluent correction is negligible for lattices of larger size. Therefore one expects that a result consistent with the theoretical prediction can be reached with $b = 0$ in formula (5) if data from large L are taken into account in the fit. Indeed with a Taylor expansion of Eq. (5) up to second order in $tL^{1/\nu}$ as well as letting $b = 0$ in Eq. (5), we arrive at $\nu = 0.7120(16)$ and $(J'/J)_c = 2.51950(3)$ using the data of $\rho_{s2}2L$ with $48 \le L \le 136$. In obtaining the results $\nu = 0.7120(16)$ and $(J'/J)_c = 2.51950(3)$, we have performed bootstrap sampling on the raw data and have carried out a large number (around 1000) of fits with a variant input for the unknown parameters[34]. The inclusion of higher order terms in the Taylor series and eliminating data of smaller L in the fits leads to compatible (and consistent) results with what we have just

[2] In addition to the confluent correction appeared in Eq. 4, there are also other corrections to scaling proportional to $L^{-2\omega}$, $L^{-\omega'}$, and so on.

[3] For example, using the full ansatz Eq. (4), a fit of the unconventional finite-size scaling (which will be introduced later) to $\rho_{s1}L$ leads to $\nu = 0.71(5)$.

obtained. The results of ν and $(J'/J)_c$ we obtain from $\rho_{s2}2L$ are shown in the first 8 rows of table 1. As indicated in table 1, the numerical values of ν determined from $\rho_{s2}2L$ are consistent with the most accurate Monte Carlo result $\nu = 0.7112(5)$ in the $O(3)$ universality class. Further, the critical points we calculate from the same observable $\rho_{s2}2L$ agrees with the known results in the literature[14] as well. The errors for $(J'/J)_c$ and ν shown in table 1 are determined by the standard deviations of the corresponding results from the fits. While the bootstrap method ocassionally would lead to underestimated errors, the bootstrap means we reach in table 1 provide a convincing evidence that our ν calculated from $\rho_{s2}2L$ agrees nicely with the expected $\nu = 0.7112(5)$. Notice the ansatz we use to fit the observable $\rho_{s2}2L$ contains either 5 or 6 unknown parameters which is reasonable. Still, one would like to see whether a value for ν consistent with its theoretical prediction can be obtained using fewer fitting coefficients. Interestingly, using the data of $\rho_{s2}2L$ very close to $(J'/J)_c$, we arrive at $\nu = 0.710(7)$ by employing a Taylor expansion of Eq. (5) up to first order in $tL^{1/\nu}$ with a fixed $(J'/J)_c = 2.51950$ and $b = 0$. The new fit we carry out contains only 3 unknown parameters. Hence we conclude that indeed our data of $\rho_{s2}2L$ can be described well by the expected $O(3)$ value for ν.

Having determined $\nu = 0.7120(16)$ using the observable $\rho_{s2}2L$, we turn to the calculations of ν based on the observables $\rho_{s1}2L$ and Q_2. First of all, we would like to reproduce the unexpected result $\nu = 0.689(5)$ found in[14]. Indeed, using the Monte Carlo data of $\rho_{s1}2L$ with L ranging from $L = 24$ to $L = 80$ (the size of $L = 80$ is similar to the largest lattice ($L = 72$) used in[14] in obtaining $\nu = 0.689(5)$), we arrive at $\nu = 0.689(3)$ and $(J'/J)_c = 2.5194(4)$, both of which are statistically consistent with those determined in[14]. Further, the ω determined from above fit is $\omega = 0.52(6)$. Finally a numerical value for ν consistent with its theoretical prediction $\nu = 0.7112(5)$ could never have been obtained using the available data for $\rho_{s1}2L$. Interestingly, the ω in Eq. (5) obtained from our fits for $\rho_{s1}2L$ are in the range $[\,0.52, 0.57\,]$, and therefore are smaller than the expected value $\omega \sim 0.78$. This implies that either the correction to scaling for $\rho_{s1}2L$ is indeed large, hence the calculations of ν using $\rho_{s1}2L$ with a subleading correction might be contaminated due to the enhanced correction, or the determination of ω from the fits is influenced by higher order terms. As a result, it will be interesting to examine whether a numerical value of ν consistent with its theoretical expectation can be determined from $\rho_{s1}2L$ by simulating lattices larger than those used here. Finally, for the observable Q_2, using the leading finite-size scaling ansatz (i.e. letting $b = 0$ in Eq. (5)), we are able to reach a value for ν which agrees even quantitatively with $\nu = 0.7112(5)$. However, the uncertainty of ν calculated from Q_2 is more than twice as large as that of ν determined from $\rho_{s2}2L$. The results for ν and $(J'/J)_c$ calculated from our finite-size scaling analysis on $\rho_{s1}2L$ and Q_2 are summarized in table 1 as well.

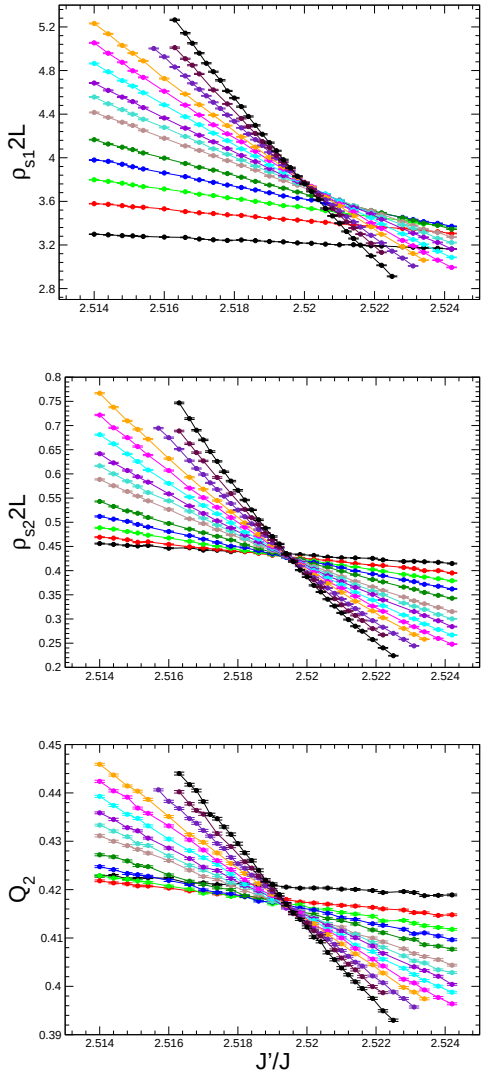

FIG. 2: Monte Carlo data of $\rho_{s1}2L$ (top), $\rho_{s2}2L$ (middle), and Q_2 (bottom).

After obtaining a result for ν which agrees quantitatively with $\nu = 0.7112(5)$, one naturally would like to see whether one can determine other exponents such as β consistent with their expected theoretical values using the relevant observables. For example, at critical point the observable $\langle (m_s^z)^2 \rangle$ should scale as $L^{-2\beta/\nu}$ for large L. Interestingly, using our data of $\langle (m_s^z)^2 \rangle$ at $J'/J = 2.5194$ we arrive at $\beta/\nu = 0.5300(18)$. Our value for β/ν is between the expected $\beta/\nu = 0.518(1)$ and the result of $\beta/\nu = 0.545(4)$ obtained in[14], implying that either the correction to scaling for $\langle (m_s^z)^2 \rangle$ is large (like that for $\rho_{s1}2L$), or the determination of β/ν is very sensitive to the exact location of $(J'/J)_c$.

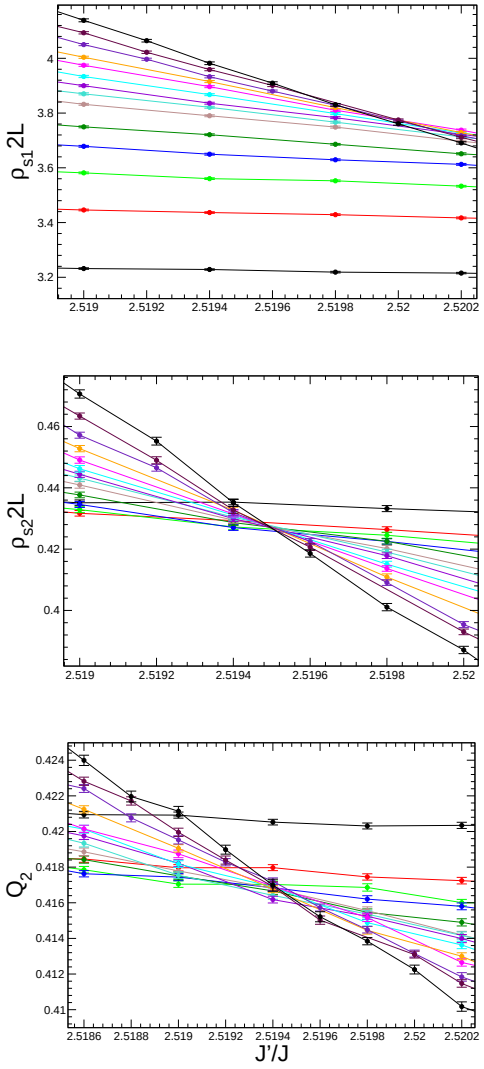

FIG. 3: Crossing of $\rho_{s1}2L$ (top), $\rho_{s2}2L$ (middle), and Q_2 (bottom) for different L near the transition.

B. Results from the unconventional finite-size scaling method

While in previous sections, with the observables $\rho_{s2}2L$ and Q_2 we are able to obtained numerical values of ν consistent with the established $O(3)$ result $\nu = 0.7112(5)$ using the conventional finite-size scaling method, it is a surprising observation that comparing to $\rho_{s2}2L$ (and Q_2 as well), $\rho_{s1}2L$ receives a much severe correction. In particular, although our results are consistent with the scenario that there is a large correction to scaling for the phase transition considered here as suggested in[26], it is unusual that we cannot reach a result for ν that agrees with $\nu = 0.7112(5)$ even with lattices as large as 136^2. This unexpected result leads one to wonder whether the conventional finite-size scaling carried out so far is the correct approach for the determination of the critical exponents and critical points of an anisotropic system. Indeed a closer look of Eq. (5), one realizes that with sufficient low temperature so that the finite temperature dependence in Eq. (5) drops out, the correct finite-size scaling for an anisotropic system is to fix the aspect ratio of winding numbers squared. The idea of this unconventional method can be justify rigorously as follows. To simplify our demonstration, let us neglect the confluent correction [4]. Notice that for anisotropic systems, the relevant aspect ratio r in (5) is the one expressed in physical units. Specifically, the finite-size scaling ansatz for anisotropic systems takes the form

$$\mathcal{O}_L(t) = g_{\mathcal{O}_L}\left(tL_1^{1/\nu}, \frac{L_1}{\xi_1}\frac{\xi_2}{L_2}\right), \tag{6}$$

where ξ_i (L_i) with $i \in \{1, 2\}$ is the correlation length (box size) in the 1- and the 2-direction, respectively. From above equation, one realizes that for anisotropic systems, the correct procedure for performing the finite-size scaling is to fix the anisotropic aspect ratio $(L_1/\xi_1)(\xi_2/L_2)$. Further, with the following relation

$$\frac{\langle W_1^2\rangle}{\langle W_2^2\rangle} = g_{12}\left(tL_1^{1/\nu}, \frac{L_1}{\xi_1}\frac{\xi_2}{L_2}\right), \tag{7}$$

one can solve for the anisotropic aspect ratio $(L_1/\xi_1)(\xi_2/L_2)$, which is then given by

$$\frac{L_1}{\xi_1}\frac{\xi_2}{L_2} = h\left(tL_1^{1/\nu}, \frac{\langle W_1^2\rangle}{\langle W_2^2\rangle}\right). \tag{8}$$

For any given renormalization group invariant quantity which satisfies the scaling properties

$$\mathcal{O}_L(t) = g_{\mathcal{O}_L}\left(tL_1^{1/\nu}, \frac{L_1}{\xi_1}\frac{\xi_2}{L_2}\right), \tag{9}$$

employing Eq. (8) will lead to

$$\mathcal{O}_L(t) = f_{\mathcal{O}_L}\left(tL_1^{1/\nu}, \frac{\langle W_1^2\rangle}{\langle W_2^2\rangle}\right). \tag{10}$$

As a consequence, the proposal of fixing the aspect ratio of spatial winding numbers squared in the simulations for anisotropic systems is correct.

After having justified the correctness of the unconventional finite-size scaling we propose here, we would like to introduce how this idea is employed in practice. First of all, one performs a trial simulation to determine a fixed value for the ratio of spatial winding numbers squared which is denoted by w_f and will be used later in all calculations. Second, instead of fixing the aspect ratio of box sizes L_1 and L_2 in the simulations as in conventional finite-size scaling studies, one then varies the variables L_1, L_2 and J'/J in order to satisfy the condition of a

[4] All the functions appeared in our derivation are smooth functions of their arguments.

J'/J	L_1	L_2	w_f/w	$(\rho_{s1})_{\rm in}$	ρ_{s1}
0.53	96	96	0.9558(33)	0.008188(22)	0.008198(7)
0.53	96	94	0.9549(32)	0.008391(21)	0.0084098(74)
0.545	90	94	0.9594(35)	0.016862(33)	0.016835(15)
0.545	90	90	0.9539(36)	0.017651(35)	0.017676(17)
0.535	98	98	0.9591(28)	0.011707(28)	0.0117297(124)
0.54	96	96	0.9592(29)	0.014838(37)	0.014846(13)
0.525	96	96	0.9503(41)	0.0072255(225)	0.0072579(66)

TABLE II: Comparison between interpolated and original values of ρ_{s1} for several data points. The data points which are used for interpolation are obtained from the simulations with $L_1 \times (L_2 + 2)$ (except the last row which is obtained from a simulation with $(L_1 + 2) \times L_2$). The inverse temperature β for these data points are fixed to $\beta J = 800$.

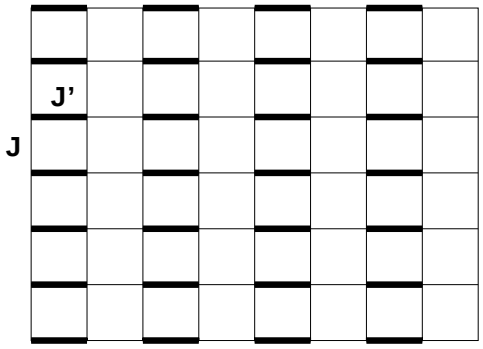

FIG. 4: Heisenberg model with a ladder pattern of anisotropy.

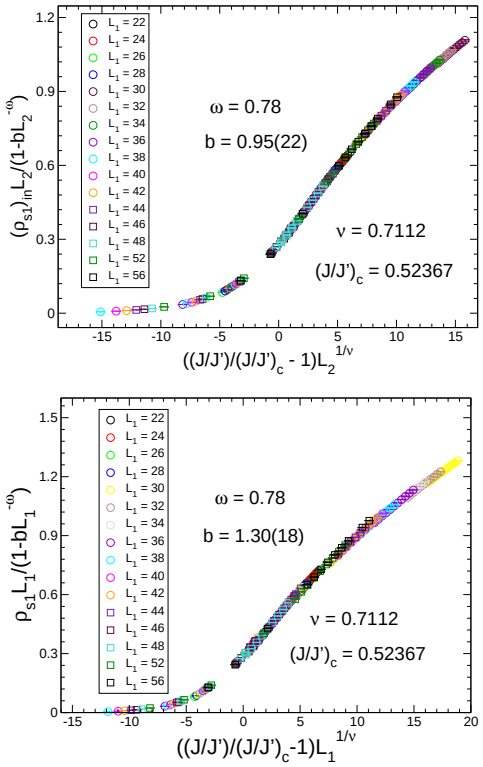

FIG. 5: Comparison between the results of data collapse using the new unconventional finite-size scaling method (upper panel) described in the text and the conventional method (lower panel) for the ladder anisotropic Heisenberg model. The result in the upper panel is obtained from simulations with box sizes $(L_2 - 6) \times L_2$, $(L_2 - 4) \times L_2$, ..., $(L_2 + 4) \times L_2$ for various values of J_2/J_1 if the interpolations from such simulations are reliable.

fixed ratio of spatial winding numbers squared. This step involves a controlled interpolation on the raw data points. In practice, for a fixed L_2 one performs simulations for a sequence $L_1 = L_2, L_2 \pm 2, L_2 \pm 4, \ldots$. The criterion of a fixed ratio of spatial winding numbers squared is reached by tuning the parameter J_2/J_1 and then carrying out a linear interpolation based on $(w/w_f)^{(-1/2)}$ for the desired observables, here w refers to the ratio of spatial winding numbers squared of the data points other than the trial one. Notice that it is natural to use L_2 in the finite-size scaling ansatz Eq. (10) both for the analysis associated with ρ_{s1} and ρ_{s2}. Although we have argue that our proposal of fixing the aspect ratio of spatial winding numbers squared is correct, it is desirable to examine the validity of this unconventional finite-size scaling method. For this purpose, we consider the quantum transition induced by dimerization for the Heisenberg model with a ladder pattern anisotropic couplings (figure 4). For $b \sim 0.95(22)$ in Eq. (4), we obtain a good data collapse for the observable $(\rho_{s1})_{\rm in} L_2$, here the subscript "in" means the data points are the interpolated one. To make sure that the step of interpolation leads to accurate results, we have carried out several trial simulations and have confirmed that the interpolated data points are reliable as long as the ratio is kept small (table 2). On the other hand, for $b = 1.30(18)$ in Eq. (4), a good data collapse is also obtained for the observable $\rho_{s1} L_1$, here ρ_{s1} are the raw data determined from the simulations directly. Figure 5 shows a comparison between the data collapse obtained by using the unconventional (upper panel) and the conventional methods (lower panel). For obtaining figure 5, we have fixed $\nu = 0.7112$, $\omega = 0.78$, and $(J/J')_c = 0.52367$, which are the established values for these quantities. As one sees in figure 5, the quality of data collapse using the unconventional method is as good as that obtained with the conventional one, thus confirming the validity of the idea to fix the ratio of winding numbers squared in order to studying the critical theory of a second order phase transition.

As demonstrated above, in general for a fixed L_2, one can vary L_1 and J'/J in order to reach the criterion of a fixed aspect-ratio of spatial winding numbers squared in the simulations. Before we proceed further, we would like to point out that to employ the unconventional finite-size scaling of a fixed aspect ratio of spatial winding numbers squared in the simulations, one needs to obtain the ground-state values for the considered observables. This is because otherwise the ratios of temporal and each of the spatial winding number squared need

to be fixed as well, which would then complicate the analysis[5]. Therefore, instead of using our Monte Carlo data obtained earlier using the relation $\beta = 2L$ in the simulations, we have carried out another set of simulations employing the condition $\beta = 5L$ in our calculations so that all the observables considered here take their ground-state values. After completing our new simulations, we proceed as follows. First of all, we calculate the ratio $\langle W_1^2\rangle/\langle W_2^2\rangle$ for the data point at $J'/J = 2.5196$ and $L = 40$ which we denote by w_f. After obtaining this number, a linear interpolation for ρ_{s1} of other data points based on $(w/w_f)^{(-1/2)}$ is performed in order to reach the criterion of a fixed ratio of spatial winding numbers squared in the simulations. The w appearing above is again the corresponding $\langle W_1^2\rangle/\langle W_2^2\rangle$ of other data points. Here a controlled interpolation similar to what we have done in studying the ladder anisotropic Heisenberg model is performed as well. Further, since large volumes data is essential for a quick convergence of ν as suggested in[25], we make sure the set of interpolated data chosen for finite-size scaling analysis contains sufficiently many points from large volumes as long as the interpolated results are reliable. A fit of the interpolated $(\rho_{s1})_{\rm in}L$ data to Eq. (5) with ω being fixed to its $O(3)$ value ($\omega = 0.78$) leads to $\nu = 0.706(7)$ and $(J/J)_c = 2.5196(1)$ for $36 \leq L \leq 64$ (figure 6). The value of ν we calculate from the fit is in good agreement with the expected $O(3)$ value $\nu = 0.7112(5)$ and the critical point $(J'/J)_c = 2.5196(1)$ we obtain is consistent with that found in[14] as well. Letting ω be a fit parameter results in consistent $\nu = 0.707(8)$ and $(J'/J)_c = 2.5196(7)$ with $\omega \sim 0.71$. Further, we always arrive at consistent results with $\nu = 0.706(7)$ and $(J'/J)_c = 2.5196(1)$ from the fits using $L > 36$ data. The numerical values of ω we reach from these fits range from 0.7 to 0.9 and are of considerable large uncertainties (comparable to the obtained ω themselves). Without a subleading correction term, we are not able to reach a good fit. These results indicate that while our data points of $(\rho_{s1})_{\rm in}L$ indeed receive correction, their quality is not precise enough to determine ω accurately. To avoid any bias, we also perform another analysis for the raw $\rho_{s1}L$ data with the same range of L and J'/J as we did for the interpolated data. By fitting this set of original data points to Eq. (5) with a fixed $\omega = 0.78$, we arrive at $\nu = 0.688(7)$ and $(J'/J)_c = 2.5197(1)$ (figure 7), both of which again agree quantitatively with those determined in[14]. Similarly, applying this unconventional finite-size scaling to ρ_{s2} would lead to a numerical value of ν consistent with $\nu = 0.7112(5)$. For instance, the ν determined by fitting $(\rho_{s2})_{\rm in}L$ to Eq. (5) is found to be $\nu = 0.706(7)$, which agrees quantitatively

[5] Interestingly, using $\rho_{s2}2L$ calculated with $\beta = 2L$ in the simulations, we arrive at $\nu = 0.7065(50)$ by employing the unconventional finite-size scaling introduced above.

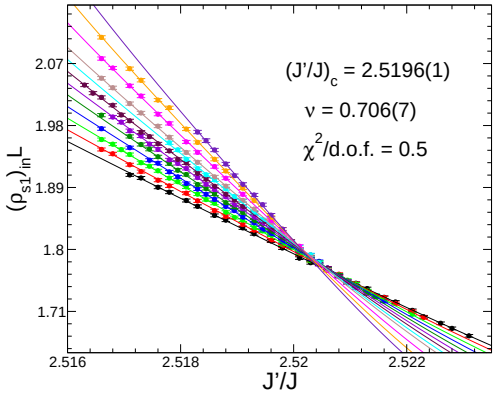

FIG. 6: Fit of interpolated $(\rho_{s1})_{\rm in}L$ data to Eq. (5). While the circles are the numerical Monte Carlo data from the simulations, the solid curves are obtained by using the results from the fit.

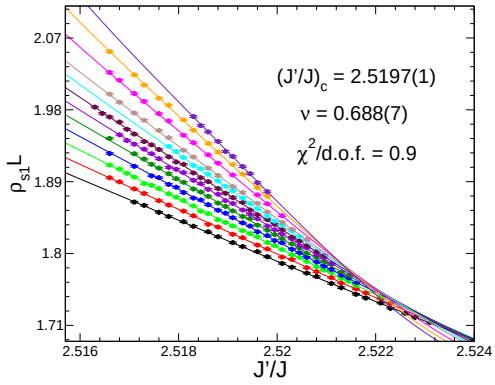

FIG. 7: Fit of original $\rho_{s1}L$ data to Eq. (5). While the circles are the numerical Monte Carlo data from the simulations, the solid curves are obtained by using the results from the fit.

with the predicted $O(3)$ value (figure 8). Finally we would like to make a comment regarding the choice of w_f. In principle one can use w_f determined from any L and from any J'/J close to $(J'/J)_c$. However it will be desirable to choose w_f such that the set of interpolated data used for analysis includes as many data points from large volumes as possible. Using the w_f obtained at $J'/J = 2.5191$ ($J'/J = 2.5196$) with $L = 40$ ($L = 44$), we reach the results of $\nu = 0.704(7)$ and $(J'/J)_c = 2.5196(1)$ ($\nu = 0.705(7)$ and $(J'/J)_c = 2.5196(1)$) from the fit with a fixed $\omega = 0.78$. These values for ν and $(J'/J)_c$ agree with what we have obtained earlier. Indeed as we will demonstrate in another investigation, the critical exponent ν determined by the idea of fixing the ratio of spatial winding number squared in the simulations is independence of the chosen reference point.

IV. DISCUSSIONS AND CONCLUSIONS

Above we have studied the critical behavior at the phase transition induced by dimerization of the spin-1/2 Heisenberg model with a spatially staggered anisotropy. Unlike the scenario suggested in[14] that an unconventional

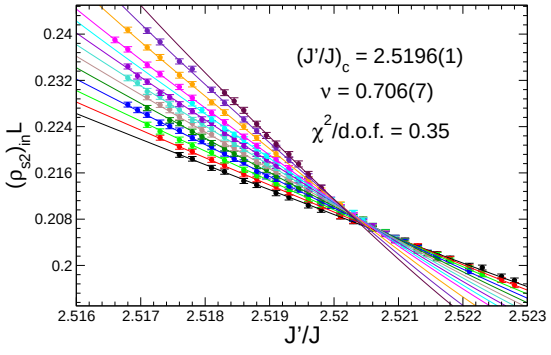

FIG. 8: Fit of interpolated $(\rho_{s2})_{\rm in}L$ data to Eq. (5). While the circles are the numerical Monte Carlo data from the simulations, the solid curves are obtained by using the results from the fit.

universality class is observed, we conclude that indeed this second order phase transition is likely in the $O(3)$ universality class. In the first part of our data analysis, we employ the conventional finite-size scaling to calculate ν and $(J'/J)_c$. Our observation of $\rho_{s2}2L$ being a good observable for determining the critical exponent ν is crucial for reading this conclusion by confirming the $O(3)$ critical exponent for this phase transition with high precision. While we do observed a large correction to scaling for the observable $\rho_{s1}2L$ as proposed in[26], the data points of $\rho_{s2}2L$ show good scaling behavior. Specifically, with $\rho_{s2}2L$, we can easily reach a highly accurate numerical value for ν consistent with the theoretical predictions without taking the confluent correction into account in the fit. The large correction to scaling observed for $\rho_{s1}2L$ in principle should influence all observables. Hence the most reasonable explanation for the good scaling behavior of $\rho_{s2}2L$ shown here is that the prefactor b in Eq. (5) for $\rho_{s2}2L$ is very small. As a result, we are able to determine the expected numerical value for ν using data of $\rho_{s2}2L$ with moderate lattice sizes. Still, a more rigorous theoretical study such as investigating whether there exists a symmetry that protects $\rho_{s2}2L$ from being affected by the large correction to scaling as suggested in[26] will be an interesting topic to explore. For example, in[26] it is argued that the enhanced correction to scaling observed for this phase transition might be due to a cubic irrelevant term which contains one-derivative in the 1-direction. The first thing one would like to understand is whether the feature of this irrelevant term, namely it contains one-derivative in the 1-direction, will lead to our observation that the large correction to scaling has little impact on $\rho_{s2}2L$. While in this study we can reach a value of ν consistent with $\nu = 0.7112(5)$, the β/ν we calculate from $\langle (m_s^z)^2 \rangle$ is statistically different from the established result of $\beta/\nu = 0.518(1)$ in the literature. Our this finding indicates that either the correction to scaling for the observable $\langle (m_s^z)^2 \rangle$ is indeed enhanced as suggested in[26], or there are some subtleties that one is not aware of when employing the technique of finite-size scaling.

After having demonstrated that the phase transition considered in this study is likely governed by the $O(3)$ universality class prediction, we examine the finite-size scaling ansatz Eq. (5) carefully due the puzzle of the anomalously large correction to scaling for $\rho_{s1}2L$ shown in figure 3. We argue theoretically that the correct strategy of performing finite-size scaling for aniostropic systems is to fix the aspect ratio of spatail winding numbers squared. Indeed, with this unconventional finite-size scaling strategy, even for the observable $\rho_{s1}L$ which receives the most severe correction to scaling, we are able to reach a numrical value for ν that is consistent quantitatively with the expected theorectial prediction $\nu = 0.7112(5)$. It will be interesting to apply a similar technique to other observables such as Binder ratios as well. However, for Binder ratios, the correction from interpolation will cancel out because of the definition of these observables. Therefore to further test the unconventional finite-size scaling method proposed here might require some new ideas. It is interesting to notice that our arguments leading to Eq. (10) seems to imply that setting $r = 1$ in Eqs. (4) and (5) when performing the finite-size scaling analysis for anisotropic systems is conceptually wrong. Still, since the conventional method of using $r = 1$ in Eqs. (4) and (5) has successfully led to correct determination of some critical exponents for anisotropic systems[10,15,25], it might be desirable to re-examine these studies to some extent.

In summary, here we present convincing numerical evidence to support that the phase transition considered in this study is well described by the $O(3)$ universality class prediction, at least for the critical exponent ν which is investigated in detail in this study. Further, whether the good scaling of $\rho_{s2}2L$ observed here is a coincidence or is generally applicable for quantum Heisenberg models with a similar spatially anisotropic pattern, remains an interesting topic for further investigation. Finally, while we have argued convincingly that the correct strategy of carrying out finite-size scaling for anisotropic systems is to fix the aspect ratio of spatial winding numbers squared, it will be of great interesting to re-examine the critical theories of other 2-d quantum Heisenberg models with spatial anisotropies in a more sophisticated manner.

V. ACKNOWLEDGEMENTS

We thank B. Smigielski for correcting the manuscript for us. Useful discussions with S. Wessel, M. Vojta, and U.-J. Wiese is acknowledged. Part of the simulations in this study were based on the loop algorithms available in ALPS library[35]. This work is partially supported by NSC (Grant No. NSC 99-2112-M003-015-MY3) and NCTS (North) of R. O. C..

* fjjiang@ntnu.edu.tw

[1] U.-J. Wiese and H.-P. Ying, Z. Phys. B **93**, 147 (1994).
[2] M. Greven, R. J. Birgeneau, and U. J. Wiese, Phys. Rev. Lett. **77**, 1865 (1996).
[3] B. B. Beard and U.-J. Wiese, Phys. Rev. Lett. **77**, 5130 (1996).
[4] A. W. Sandvik, Phys. Rev. B **56**, 11678 (1997).
[5] M. Troyer, M. Imada, and K. Ueda, J. Phys. Soc. Jpn. **66**, 2957 (1997).
[6] Y. J. Kim, M. Greven, U. J. Wiese, and R. J. Birgeneau, Eur. Phys. J. B **4**, 291 (1998).
[7] J. K. Kim and M. Troyer, Phys. Rev. Lett. **80**, 2705 (1998).
[8] A. W. Sandvik, Phys. Rev. Lett. **83**, 3069 (1999).
[9] Y. J. Kim and R. J. Birgeneau, Phys. Rev. B **62**, 6378 (2000).
[10] M. Matsumoto, C. Yasuda, S. Todo, and H. Takayama, Phys. Rev. B **65**, 014407 (2001)
[11] L. Wang, K. S. D. Beach, and A. W. Sandvik, Phys. Rev. B **73**, 014431 (2006).
[12] F.-J. Jiang, F. Kämpfer, M. Nyfeler, and W.-J. Wiese, Phys. Rev. B **78**, 214406 (2008).
[13] A. F. Albuquerque, M. Troyer, and J. Oitmaa, Phys. Rev. B **78**, 132402 (2008).
[14] S. Wenzel, L. Bogacz, and W. Janke, Phys. Rev. Lett. **101**, 127202 (2008).
[15] S. Wenzel and W. Janke, Phys. Rev. B **79**, 014410 (2009).
[16] S. Chakravarty, B. I. Halperin, and D. R. Nelson, Phys. Rev. Lett. **60**, 1057 (1988).
[17] A. V. Chubukov, S. Sachdev, and J. Ye, Phys. Rev. B **49**, 11919 (1994).
[18] S. Sachdev, *Quantum Phase Transitions* (Cambridge University Press, Cambridge, 1999).
[19] M. Vojta, Rep. Prog. Phys. **66**, 2069 (2003).
[20] F.-J. Jiang, Phys. Rev. B **83**, 024419 (2011).
[21] F.-J. Jiang and U.-J. Wiese, Phys. Rev. B **83**, 155120 (2011).
[22] T. Pardini, R. R. P. Singh, A. Katanin and O. P. Sushkov, Phys. Rev. B **78**, 024439 (2008).
[23] F.-J. Jiang, F. Kämpfer, and M. Nyfeler, Phys. Rev. B **80**, 033104 (2009).
[24] M. Campostrini, M. Hasenbusch, A. Pelissetto, P. Rossi, and E. Vicari, Phys. Rev. B **65**, 144520 (2002).
[25] F.-J. Jiang and U. Gerber, J. Stat. Mech. P09016 (2009).
[26] L. Fritz et al., Phys. Rev. B **83**, 174416 (2011)
[27] H. G. Evertz, G. Lana, and M. Marcu, Phys. Rev. Lett. **70**, 875 (1993).
[28] H. G. Evertz, Adv. Phys. **52**, 1 (2003).
[29] M. E. Fisher and M. N. Barber, Phys. Rev. Lett. **28**, 1516 (1972).
[30] E. Brézin, J. Phys. (Paris) **43**, 15 (1982).
[31] M. N. Barber, in *Phase Transitions and Critical Phenomena*, ed. C. Domb (Academic, New York, 1983), Vol. 8.
[32] E. Brézin and J. Zinn-Justin, Nucl. Phys. B **257**, 867 (1985).
[33] M. P. A. Fisher, P. B. Weichman, G. Grinstein, and D. S. Fisher, Phys. Rev. B **40**, 546 (1989).
[34] B. Efron and G. Gong, Am. Stat. **37**, 36 (1983).
[35] A. F. Albuquerque et. al, Journal of Magnetism and Magnetic Material 310, 1187 (2007).